Title: Systemic Calcitonin Gene-Related Peptide (CGRP) modifies auditory and vestibular endorgan electrical potentials, and increases auditory and vestibular hypersensitivities: Implications for vestibular migraine

Abbreviated Title: CGRP's effect on endorgan and behavior

Authors: Shafaqat M. Rahman[1], Benjamin Liang[1], Stefanie Faucher[1], Elana Fine[1], Raajan Jonnala[1], Joseph C. Holt[2,3], Choongheon Lee[3], Anne E. Luebke[1,2*]

Affiliations:

[1]University of Rochester, Department of Biomedical Engineering, Rochester, NY 14627

[2]University of Rochester Medical Center, Department of Neuroscience, Del Monte Institute of Neuroscience, Rochester, NY 14642

[3]University of Rochester Medical Center, Department of Otolaryngology, Rochester, NY 14642

*Corresponding author: Anne E. Luebke, aluebke@ur.rochester.edu

Number of Pages: 21

Number of Figures: 3

Number of Tables: 0

Number of words for Abstract: 229

Number of words for Introduction: 343

Number of words for Discussion: 581

Conflict of interest statement: The authors declare no competing financial interests.

Acknowledgments: This work was fully supported by NIH R01DC017261.

Abstract:

Migraine is a severe and chronic neurological disorder that affects ~18% of people worldwide, the majority female (3:1). It is characterized by recurrent, debilitating headaches and heightened sensory sensitivities to stimuli, and migraineurs may also experience a heightened motion sensitivity that leads to episodes of vertigo and imbalance, termed vestibular migraine (VM). Calcitonin Gene-Related Peptide (CGRP) is implicated in migraine and is believed to act on brain meninges, midbrain, or brainstem, and CGRP-based therapeutics have shown efficacy for migraine treatment. However, CGRP also signals at efferent synapses of the cochlea and vestibular endorgans, and it is unclear if exogenous CGRP can modulate inner ear function and cause heightened behavioral responses consistent with VM. In C57BL6/J mice, we tested if intraperitoneally (IP) delivered CGRP can modulate endorgan potentials to sound [via auditory brainstem responses (ABRs)]and jerk stimulus [via vestibular sensory evoked potentials (VsEPs)]. We also assessed behavioral measures of phonophobia [acoustic startle reflex (ASR)] and imbalance [postural sway center of pressure (CoP)] after IP CGRP, and observed female mice exhibit heightened sensitivities to IP CGRP in all assays, while male mice showed similar auditory sensitivity, and endorgan effects, but no postural sway changes. In conclusion, we show that systemically delivered CGRP modulates the activity of the auditory and vestibular endorgans; and elicits some behavioral effects that are sex-specific, and are consistent with symptoms in a disorder like VM.

Significance statement:

Calcitonin Gene-Related Peptide (CGRP) has been implicated in migraine, and CGRP-based therapeutics have shown efficacy in the treatment of migraine headaches. Yet, CGRP is also present in efferent synapses of the inner ear, and it is not clear if increases in systemic CGRP can act directly on inner ear endorgans, and modify corresponding behavioral responses. In this study, we determined systemic CGRP changes both cochlear and vestibular endorgan potentials, and produced behaviors suggestive of phonophobia, and increased postural sway. Peripheral changes in auditory and vestibular compound action potentials following systemic CGRP, suggest systemic CGRP can act directly on the inner ear, which opens new therapeutic targets to treat migraine with vertigo.

50

51 **Introduction:**

52 Migraine is a debilitating chronic neurological disorder that is listed by the World Health Organization
53 (WHO) as the most debilitating neurological disorder worldwide and is estimated to affect 18% of
54 women and 6% of men (Goadsby, Lipton, and Ferrari 2002; Lipton et al. 2007). About 42% of
55 migraineurs have a vestibular component causing balance problems and dizziness (Kuritzky, Toglia,
56 and Thomas 1981; Neuhauser et al. 2001; Neuhauser 2007, 2009), termed vestibular migraine (VM).
57 VM is a major cause of vertigo in dizziness clinics (Kayan and Hood 1984), and patients with migraine,
58 and especially VM, exhibit a heightened sense of sound (Ashkenazi et al. 2009; Lopez-Escamez et al.
59 2014), yet despite migraine and VM's prevalence, the pathophysiology remains uncertain (Lempert et
60 al. 2022; Lempert et al. 2012).

61

62 Calcitonin gene-related peptide (CGRP) is hypothesized to play a role in sensory hypersensitivity in
63 migraine (Russo 2015). In patients, CGRP levels are elevated during migraine, and normalization of
64 CGRP levels is associated with the relief of headache pain which is thought to act at either brain
65 meninges, or the trigeminal system (Goadsby, Lipton, and Ferrari 2002; Juhasz et al. 2005; Lassen et
66 al. 2002). However, CGRP also signals at efferent synapses of the cochlea and vestibular endorgans,
67 so we wondered if the elevated CGRP levels of migraine could affect the inner ear directly. To that
68 end, we modeled the increase in CGRP during migraine, by a systemic intraperitoneal (IP) injection, to
69 determine if systemic CGRP can modulate activity of these endorgans (Dickerson et al. 2016; Luebke
70 et al. 2014; Maison et al. 2003). We were also interested in knowing if increases in systemic CGRP
71 can cause behaviors suggestive of heightened auditory and vestibular sway consistent with VM.

72

73 In this study, we tested wildtype C57BL6/J mice to determine if there is a change in endorgan potentials
74 to sound (measured using auditory brainstem responses –ABRs) and jerk stimulus [measured using
75 vestibular stimulus evoked potentials (VsEPs)] after a CGRP injection. We also assessed
76 corresponding behavioral measures of phonophobia (acoustic startle reflex – ASR) and imbalance
77 (postural sway) after systemic CGRP injection.

78

79 **Methods:**

80 Animals: C57BL6/J mice were obtained from Jackson Laboratories (JAX #664) and were housed under
81 a 12-hour day/night cycle under the care of the University Committee on Animal Resources (UCAR) at
82 the University of Rochester. Mice are housed together in cages (max 5 mice per cage) with *ad libitum*
83 access to food, water, and bedding material. Equal numbers of male and female mice were tested and
84 a total of 82 mice (41 M/ 41F) were used for these studies, which were powered sufficiently to detect
85 male/female differences. Before experimentation on each testing day, mice were equilibrated in the
86 testing room controlled for an ambient temperature between 22-23°C for at least 30 minutes, and
87 remained in this room until completion of experiments. Injections occurred after the equilibration period.
88 Mice used during behavioral experiments were returned to the vivarium, while mice used for ABR/VsEP
89 experiments were euthanized after testing. Mice tested were between 2.3 - 6 months of age. This age
90 range in mice correlates to 20-30 years in humans, which is within the age range that patients with
91 migraine develop symptoms (Lessem 2018). All animal procedures were approved by the University of
92 Rochester's IACUC committee and performed in accordance with the standards set by the NIH.

93

94 VsEP and ABR Protocol: C57BL/6 mice were anesthetized with IP urethane/xylazine (1.2 g/kg/20
95 mg/kg). VsEP and ABR recording methods have been described in detail elsewhere (Lee, Holt, and
96 Jones 2017). Briefly, to record VsEP and ABR, subcutaneous electrodes were placed on the midline
97 over the nuchal crest (G1), behind the right pinna (G2), and on the hip (ground). A noninvasive head
98 clip was used to secure the mouse's head to an electromechanical shaker. During VsEPs, the shaker
99 delivered a transient (jerk) head translation in the naso-occipital axis (± X). To confirm the absence of
100 auditory responses during VsEP testing, a binaural forward masker (intensity: 92 dB SPL; bandwidth:
101 50~50 kHz) was presented with the use of a free-field speaker (FF1, TDT). For ABR recordings, the
102 same electrodes were used to record ABRs, which were evoked by a single rectangular voltage pulse
103 of 0.03 ms duration (corresponding to 33 kHz cut-off frequency). These click stimuli were presented via
104 a free-field speaker, which was the same driver for acoustic masking during the VsEP recording. A
105 noninvasive rectal thermometer or thermistor was used to monitor the animals' core temperature at

106 38.0 ± 0.2°C. The standard signal averaging technique described in previous studies (Lee, Holt, and
107 Jones 2017) was used to record both VsEP and ABR, as shown in Fig. 1A. Recordings of both VsEP
108 and ABR were made in a soundproof booth. Both VsEPs at maximal intensity +6 dB re: 1 g/ms and
109 ABRs at maximal intensity 100 dB SPL, were recorded as a stable baseline before a single IP injection
110 of either vehicle control (PBS) or 0.1 mg/kg CGRP was given. Control amplitude and latencies are
111 depicted as the averages of the 2-3 measurements taken during baseline before injection. Following
112 single IP injection of either vehicle or CGRP, VsEP and ABR recordings were continuously measured
113 where significant shifts in VsEP and ABR responses were first observed in 10 mins and reaching a
114 plateau within 15 mins of drug injection (post-CGRP; data not shown). Thus, amplitudes and latencies
115 depicted as post-saline/post-CGRP are averages of the 2-3 measurements taken after 20-30 min post-
116 injections.
117
118 Drug administration: Injections were performed intraperitoneally (IP) with a fine gauge (30ga) insulin
119 syringe. Dulbecco PBS served as the vehicle control. IP CGRP was prepared at 0.1 mg/kg (rat α-
120 CGRP, Sigma). Injection volumes were calibrated so that each animal received 1 injection per testing
121 day at ~100 ul. For behavioral experiments, mice were tested ~20 minutes after IP delivery of either
122 vehicle or CGRP.
123
124 Behavioral test of phonophobia: Acoustic startle reflex (ASR)
125 To assess behavioral phonophobia or heightened sound sensitivity, we made use of the acoustic startle
126 response (ASR). Experiments were conducted within a sound-attenuating room (IAC, Bronx, NY) with
127 Sonex foam lined walls. Mice were placed individually in a wire-mesh cage, 5 cm wide, 7 cm long, and
128 4 cm high, having free sound penetration. The testing cage was oriented so that the mouse's head
129 faced a Tucker Davis ES2 electrostatic speaker (Masker Speaker) located 46 cm directly in front of the
130 mouse's head (60dB BBN). The startle speaker was a Radio Shack tweeter that was suspended 15 cm
131 above the mouse (80-130 dB). The acoustic startle speaker and its supports, the pedestal, acrylic shelf,
132 and the table on which the apparatus was placed were all covered with echo absorbing foam and
133 carpeting. Force of the acoustic startle response (ASR) was transduced by an accelerometer and

134 amplitude scored as integrated root mean square voltage for 100 ms after delivery of the ASR.
135 Experimental stimuli were controlled, and responses were recorded using custom MATLAB
136 (MathWorks) software. We tested acoustic startle series in quiet and in noise. There were 12 conditions
137 in this session with startle stimuli ranging from 80 to 130 dB SPL, delivered in silence or in a continuous
138 background noise. Background noise, when present, was on for the duration of the inter-trial interval
139 and broadcast from the masker speaker, as shown schematically in Fig. 2.
140
141 Behavioral test of postural sway
142 Postural sway was measured as a correlate for static balance. Mice were weighed and placed on a
143 force plate designed to measure forces in the X, Y, Z and its moments in the XY, YZ, and XZ directions.
144 We used the AMTI Biomechanics Force platform (model HEX6x6) and AMTI automated acquisition
145 software to obtain forces and moments and then MATLAB code was used to calculate Center of
146 Pressure (CoP) measures based on a generating a 95% confidence ellipse enclosing 95% of the CoP
147 trajectory values recorded in a single trial. During a given test, a mouse was first allowed to freely
148 maneuver on the force plate for 2-5 minutes to acclimate to the novel environment. An accessory
149 plexiglass guard was placed around the force plate to prevent animals from moving off the test plate.
150 After acclimation, ~ 10 baseline measurements were taken of the mouse with each measurement
151 indicating a CoP area (resolution per CoP measurement: 300 samples per second). These
152 measurements were taken when the mouse showed no movement and its four paws were touching the
153 force platform. To assess the effect of a vestibular challenge (VC), the mouse was then subjected to a
154 constant orbital rotation, 125 rpm for 5 minutes, and was placed back onto the force platform. After a
155 five-minute recovery period, an additional 10 measurements were recorded of the mouse's sway to
156 determine effect of the vestibular challenge (post VC measures), as schematized in **Fig. 3**. Mice were
157 first tested after systemic delivery of IP vehicle (20 min after injection), with sway measured both before
158 and after vestibular challenge. Four days after vehicle control testing, the same mice were injected with
159 IP CGRP and were tested again 20 minutes after injection (timing correlated with endorgan potential
160 changes). While systemic CGRP's effect is believed to dissipate two to three hours post–injection, we
161 retested after four days to eliminate any residual dizziness due to VC or lingering effects of CGRP. In

162 some animals we staggered sequence of IP injections, injecting CGRP followed by vehicle testing. We
163 also injected vehicle 2x to assess test/retest reliability and saw no differences (data not shown). In
164 certain testing conditions, mice exhibited unreasonably large CoP values (> 15 cm^2) that suggested that
165 they were either moving during the time of measurement or that they were at the edge of the force
166 plate, and those values were excluded based on a 10% ROUT analysis (GraphPad Prism 9.0). Yet,
167 even with values excluded, a minimum of eight different 95% ellipses were computed per mouse, per
168 condition tested.
169
170 Statistical Analyses
171 All statistical analyses were conducted in GraphPad Prism 9.0. Repeated measure ANOVA (RM-
172 ANOVA) and paired t-tests were the primary statistical tools. Bonferroni and Tukey multiple
173 comparisons test were used to assess for differences between treatment groups. Significance was
174 set at $p < 0.05$ for all analyses.
175
176 **Results:**
177 IP CGRP's Effects on ABR:
178 Representative traces are shown for ABR recordings in female and male C57BL6/J mice **(Fig. 1B-1C)**.
179 A 2-way RM ANOVA assessing the factors - IP CGRP and sex - showed IP CGRP's effects to be
180 significant on wave 1 ABR amplitudes (*F (1, 12) = 11.81; p = 0.005*). Female control ABR amplitudes (n
181 = 6) were computed to be 3.60 ± 0.22 μV but were increased to 4.28 ± 0.25 μV after IP CGRP
182 (*Bonferroni*, *p = 0.007*). Likewise, male control amplitudes (n = 7) were computed to be 4.31 ± 0.5 μV
183 and increased to 4.66 ± 0.44 μV after IP CGRP, but were not deemed statistically significant **(Fig. 1F)**.
184 Wave 1 ABR amplitudes were normalized so that post-CGRP measurements highlight the change in
185 amplitude from their respective control measurements (Δ wave1 amplitude*),* and both sexes were
186 additionally pooled in this depiction **(Fig. 1G)**. When both sexes are pooled (n = 13), a statistically
187 significant Δ increase of 0.50 ± 0.13 μV was observed in wave 1 amplitudes due to IP CGRP (*paired t-*
188 *test; t, df = 3.9,12; p = 0.002*). Wave 2-1 ABR latencies were calculated as the difference between P2
189 and P1 latencies for control and post-CGRP; however, no significant differences were observed in

190 latency differences **(Fig. 1H).** A separate group of mice was tested for the effects of PBS as the vehicle
191 (n = 4), but no significant differences were seen in Δ wave1 amplitude or latency differences between
192 control and post-vehicle ABR (Δ wave1 amplitude $_{vehicle - control}$ = -0.19 ± 0.21 μV).
193
194 <u>IP CGRP's Effects on VsEPs:</u>
195 Similar to ABR tests, representative traces are shown for VsEP recordings in females and males (**Fig.**
196 **1D-1E).** A 2-way RM ANOVA (factors: CGRP, sex) showed CGRP's effects to be significant on P1-N1
197 VsEP amplitudes (*F (1, 11) = 16.9; p = 0.002*). Female P1-N1 VsEP control amplitudes (n = 6) were
198 computed to be 0.68 ± 0.06 μV but were reduced to 0.55 ± 0.06 μV after IP CGRP, however, this
199 reduction was not deemed statistically significant **(Fig. 1I)**. Likewise, male P1-N1 VsEP control
200 amplitudes (n = 8) were computed to be 0.95 ± 0.10 μV but were reduced significantly to 0.76 ± 0.10 μV
201 after IP CGRP (*Bonferroni*, *p = 0.02*). P1-N1 amplitudes were normalized so that post-CGRP
202 measurements highlight the change in amplitude from their respective control (Δ P1-N1 amplitude*),* and
203 both sexes were additionally pooled (**Fig. 1J**). When pooling all animals (n = 14), a significant Δ
204 reduction of -0.16 ± 0.04 uV in P1-N1 amplitude is observed due to IP CGRP (*paired t-test; t, df = 3.63,*
205 *13; p = 0.003*).
206
207 P1, N1, and P2 latencies were also assessed for VsEPs, and these latencies are depicted as mean ±
208 SEM for females and males during control and post-CGRP tests **(Fig. 1K).** While no significant
209 differences were observed due to IP CGRP, modest delays in P1 were observed due to IP CGRP in
210 either sex. IP CGRP increased female P1 by 26.6 microseconds and male P1 by 22.5 microseconds
211 compared to P1 control latencies. IP CGRP also increased female N1 by 30 microseconds but had no
212 effect on Male N1. However, these latency changes were not statistically significant. Comparatively in
213 mice treated with IP vehicle, no significant P1-N1 amplitude or latency differences were observed
214 between control and post-vehicle VsEP (Δ P1-N1 amplitude $_{vehicle - control}$ = -0.03 ± 0.08 μV).
215
216 <u>CGRP's effect on sound sensitivity</u>

217 Our sound sensitivity measure in the mouse model makes use of the acoustic startle response (ASR) in
218 quiet and in background noise. Mice were assessed for the effects of IP CGRP as compared to IP
219 vehicle on their baseline. The ASR experimental setup is illustrated in **Fig. 2 A** (quiet) and **Fig. 2D**
220 (background noise 60 dB). In both IP vehicle and IP CGRP injected animals, an increase in ASR was
221 detected with increasing loudness of the startle stimulus (ES). All animals tested exhibited robust
222 startle responses. When ASR was tested after IP CGRP injection and compared to IP vehicle, all
223 animals exhibited reduced ASR thresholds in both quiet and noise. IP CGRP significantly increased
224 sound sensitivity to the startle stimulus in quiet (**Fig. 2 B, C**) and in background noise (**Fig. 2 E, F**) in
225 both female and male mice at all sound levels ($p<0.0001$).
226
227 <u>CGRP's and VC's effects on Postural Sway</u>
228 Mice were assessed for postural sway by determining center of pressure (CoP) area. An experimental
229 timeline is shown in **Fig. 3A**. Twenty minutes after delivery of IP vehicle and without a vestibular
230 challenge (VC), group averages of 95% ellipse areas were computed to be 0.5 ± 0.06 cm^2 for females
231 and 0.4 ± 0.04 cm^2 for males **(Fig. 3B and C).** For comparison, a deadweight (toy mouse) was also
232 measured on the force platform, and its average 95% ellipse area was computed to be 0.02 ± 0.0005
233 cm^2 **(Fig. 3D).** A different cohort of mice (10M/ 10F) was assessed for a test-retest of 95% ellipse areas
234 after IP vehicle delivery, and testing occurred four days apart. No significant differences were seen in
235 either sex during the test-retest (mean ± $SE_{\text{test-retest difference}}$ for females = 0.10 ± 0.3 cm^2 *(Bonferroni, $p >$*
236 *0.99)* and males = -0.14 + 0.3 cm^2 *(Bonferroni, $p > 0.99$)*). A 3-way ANOVA was used to assess the
237 factors of sex, CGRP, and VC on 95% ellipse areas and is graphically depicted via a violin plot **(Fig.**
238 **3E).** Significant differences were seen across the following factors: sex ($F(1.00, 22.00) = 25.26, p <$
239 0.0001) and CGRP ($F(1.00, 22.00) = 4.67, p = 0.04$). The effects of VC were trending ($F(1.00, 22.00)$
240 $= 2.93, p = 0.1$). Tukey post-hoc analysis was used to observe differences in specific comparisons
241 across the three factors. An increase was seen in 95% ellipse due to the VC in female mice treated with
242 IP vehicle *($p = 0.053$)*, as shown in the before/after plot (**Fig. 3F**). However, before the VC (pre-VC), in
243 females but not males, IP CGRP induced significant increases in CoP ellipse areas by 0.94 ± 0.23 cm^2
244 ($p = 0.01$) as seen in the before-after plot **(Fig. 3G).** When looking at sex differences, they were not

245 observed after delivery of IP vehicle. However, during the pre-VC tests after IP CGRP, females had
246 higher 95% ellipse areas compared to males by 0.96 ± 0.19 cm^2 (*p = 0.007*).
247 The major and minor axes of 95% ellipse areas were also analyzed with 3-way ANOVA and
248 post-hoc analysis through Tukey's multiple comparisons test (**Fig. 3H and I**). The major and minor axes
249 lengths serve as correlates for anteroposterior (AP) and mediolateral (ML) sway magnitudes. In pre-VC
250 female values, IP CGRP increased AP ellipse lengths by 0.49 + 0.10 cm compared to their IP vehicle
251 tests (*p = 0.005*). Also, in IP vehicle-treated females, there was an increase in AP ellipse lengths due to
252 the VC, but this was trending (*t (p = 0.056)*), and IP CGRP-treated females exhibited greater AP
253 lengths compared to males during pre-VC testing by 0.57 + 0.10 cm, (*p = 0.0002*). When observing ML
254 sway, like AP sway, IP vehicle-treated females showed increased ML lengths due to VC, but this was
255 trending (*t (p = 0.07*)). Additionally, IP-CGRP-treated females exhibited increased ML ellipse lengths
256 compared to their IP vehicle response by 0.12 + 0.03 cm, (*p = 0.02*). No other significant changes were
257 observed in AP and ML sway.
258
259 **Discussion:**
260 Using electrophysiological techniques (ABR/VsEP), we observed that systemic, intraperitoneally
261 delivered CGRP modulates endorgan function in the inner ear with a maximum ~20- 30 minutes after
262 injection. Exogenous CGRP increases wave 1 amplitudes of the ABR but reduces VsEP P1-N1
263 amplitudes, suggesting that at least one action of systemic CGRP is at the efferent signaling sites of the
264 auditory and vestibular periphery. We did not further characterize wave 2 and later peaks of
265 amplitudes or latencies, as we were primarily interested in wave 1/P1-N1 as an indicator of sensory
266 processing changes at the periphery.
267 Furthermore, we observed that systemic CGRP - during this 20–30-minute time - increased
268 sound sensitivity in both male and female wildtype C57BL6/J mice, whereas it only increased postural
269 sway in female mice.
270 A few studies in animal models have provided additional evidence for CGRP's role in vestibular
271 dysfunction and sound sensitivity. Consistent with current VsEP results where we observed delays in
272 VsEP latencies due to systemic CGRP (though not statistically significant), the loss of αCGRP In

273 transgenic mouse lines significantly enhanced activation timing of the macular sensors, through
274 changes at the endorgan level (Jones et al. 2018). Intracerebral-ventricular (ICV) injection of
275 nitroglycerin (NTG) caused impaired balance beam walking in rats, and immunohistochemistry
276 detected more CGRP expression in the vestibular nucleus of the NTG rat model than was observed in
277 control rats. The administration of a CGRP-receptor antagonist (olcegepant-BIBN4096BS) was shown
278 to be effective in alleviating impaired balance beam walking (Zhang et al. 2020; Tian et al. 2022). In
279 addition, a recent study suggested CGRP has an excitatory role in the auditory nerve response, as
280 intra-cochlear CGRP infusion was shown to enhance spontaneous and sound-driven auditory nerve
281 activity in guinea pigs, in comparison to CGRP-null mice where a loss of nerve activity excitation was
282 observed (Le Prell et al. 2021; Allen and Luebke 2017). Thus, the auditory nerve may be hyper-
283 sensitized to CGRP's effects during a migraine.

284 Peripheral effects of systemic CGRP administration on VsEP responses is somewhat surprising,
285 as the post-CGRP injection VsEP potentials were reduced and it is unclear why. However, this
286 observation is relevant to VM, which is characterized by sensory misintegration to, and thus reduced
287 vestibular sensitivity that occurs concurrently with a heightened auditory sensitivity may provide a
288 basis for the occurrence of these symptoms.

289 Additionally, it is unclear why we did not find significant changes in males during postural sway
290 testing. While more males exhibited significant changes in their VsEP measures, we presume the lack
291 of CGRP-induced behavioral effects on sway may be due to other postural compensatory mechanisms
292 present in male mice. Yet, we did discover a robust sex difference when assessing mouse postural
293 sway, as female mice were much more affected than their male counterparts to injected CGRP.
294 Similar female-specific sexual dimorphism has been observed in other animal assays assessing
295 CGRP's effects in migraine but we are the first to show such differences in preclinical migraine
296 correlates of postural sway (Recober et al. 2009; Paige et al. 2022).

297 Small molecule blockers of the CGRP receptor ‘gepants’ have been shown to enter the
298 periphery, brainstem, and midbrain areas. Future studies will determine if blocking CGRP receptor
299 signaling by small molecules (‘gepants”) or by larger monoclonal blocking antibodies [that may or may
300 not cross blood brain barrier (BBB), but have been shown to be permeable to various peripheral

301 ganglia] can reduce these sound and imbalance sensitivities present after systemic CGRP injection

302 (Noseda et al. 2020; Tian et al. 2022; Zhang et al. 2020).

303

References:

Allen, Paul D., and Anne E. Luebke. 2017. 'Reflex Modification Audiometry Reveals Dual Roles for Olivocochlear Neurotransmission', *Frontiers in Cellular Neuroscience*, 11.

Ashkenazi, A., A. Mushtaq, I. Yang, and M. L. Oshinsky. 2009. 'Ictal and interictal phonophobia in migraine-a quantitative controlled study', *Cephalalgia*, 29: 1042-8.

Dickerson, I. M., R. Bussey-Gaborski, J. C. Holt, P. M. Jordan, and A. E. Luebke. 2016. 'Maturation of suprathreshold auditory nerve activity involves cochlear CGRP-receptor complex formation', *Physiol Rep*, 4.

Goadsby, P. J., R. B. Lipton, and M. D. Ferrari. 2002. 'Migraine--current understanding and treatment', *N Engl J Med*, 346: 257-70.

Jones, S. M., S. Vijayakumar, S. A. Dow, J. C. Holt, P. M. Jordan, and A. E. Luebke. 2018. 'Loss of alpha-Calcitonin Gene-Related Peptide (alphaCGRP) Reduces Otolith Activation Timing Dynamics and Impairs Balance', *Front Mol Neurosci*, 11: 289.

Juhasz, G., T. Zsombok, B. Jakab, J. Nemeth, J. Szolcsanyi, and G. Bagdy. 2005. 'Sumatriptan causes parallel decrease in plasma calcitonin gene-related peptide (CGRP) concentration and migraine headache during nitroglycerin induced migraine attack', *Cephalalgia*, 25: 179-83.

Kayan, A., and J. D. Hood. 1984. 'Neuro-otological manifestations of migraine', *Brain*, 107 (Pt 4): 1123-42.

Kuritzky, A., U. J. Toglia, and D. Thomas. 1981. 'Vestibular function in migraine', *Headache*, 21: 110-2.

Lassen, L. H., P. A. Haderslev, V. B. Jacobsen, H. K. Iversen, B. Sperling, and J. Olesen. 2002. 'CGRP may play a causative role in migraine', *Cephalalgia*, 22: 54-61.

326 Le Prell, Colleen G., Larry F. Hughes, David F. Dolan, and Sanford C. Bledsoe. 2021. 'Effects of
327 Calcitonin-Gene-Related-Peptide on Auditory Nerve Activity', *Frontiers in Cell and*
328 *Developmental Biology*, 9.

329 Lee, C., J. C. Holt, and T. A. Jones. 2017. 'Effect of M-current modulation on mammalian vestibular
330 responses to transient head motion', *J Neurophysiol*, 118: 2991-3006.

331 Lempert, T., J. Olesen, J. Furman, J. Waterston, B. Seemungal, J. Carey, A. Bisdorff, M. Versino, S.
332 Evers, A. Kheradmand, and D. Newman-Toker. 2022. 'Vestibular migraine: Diagnostic criteria1',
333 *J Vestib Res*, 32: 1-6.

334 Lempert, T., J. Olesen, J. Furman, J. Waterston, B. Seemungal, J. Carey, A. Bisdorff, M. Versino, S.
335 Evers, and D. Newman-Toker. 2012. 'Vestibular migraine: diagnostic criteria', *J Vestib Res*, 22:
336 167-72.

337 Lessem, Sarah E. 2018. "QuickStats: Percentage of Adults Who Had a Severe Headache or Migraine
338 in the Past 3 months, by Sex and Age Grou - National Health Interview Survey, United States,
339 2018." In *Morbidity and Mortality Weekly Report (MMWR)*, edited by National Center for Health
340 Statistics.

341 Lipton, R. B., M. E. Bigal, M. Diamond, F. Freitag, M. L. Reed, W. F. Stewart, and Ampp Advisory
342 Group. 2007. 'Migraine prevalence, disease burden, and the need for preventive therapy',
343 *Neurology*, 68: 343-9.

344 Lopez-Escamez, J. A., J. Dlugaiczyk, J. Jacobs, T. Lempert, R. Teggi, M. von Brevern, and A. Bisdorff.
345 2014. 'Accompanying Symptoms Overlap during Attacks in Meniere's Disease and Vestibular
346 Migraine', *Front Neurol*, 5: 265.

347 Luebke, A. E., J. C. Holt, P. M. Jordan, Y. S. Wong, J. S. Caldwell, and K. E. Cullen. 2014. 'Loss of
348 alpha-calcitonin gene-related peptide (alphaCGRP) reduces the efficacy of the Vestibulo-ocular
349 Reflex (VOR)', *J Neurosci*, 34: 10453-8.

350 Maison, S. F., R. B. Emeson, J. C. Adams, A. E. Luebke, and M. C. Liberman. 2003. 'Loss of alpha
351 CGRP reduces sound-evoked activity in the cochlear nerve', *J Neurophysiol*, 90: 2941-9.

352 Neuhauser, H. K. 2007. 'Epidemiology of vertigo', *Curr Opin Neurol*, 20: 40-6.

353 ———. 2009. '[Epidemiology of dizziness and vertigo]', *Nervenarzt*, 80: 887-94.

354 Neuhauser, H., M. Leopold, M. von Brevern, G. Arnold, and T. Lempert. 2001. 'The interrelations of
355 migraine, vertigo, and migrainous vertigo', *Neurology*, 56: 436-41.

356 Noseda, R., A. J. Schain, A. Melo-Carrillo, J. Tien, J. Stratton, F. Mai, A. M. Strassman, and R.
357 Burstein. 2020. 'Fluorescently-labeled fremanezumab is distributed to sensory and autonomic
358 ganglia and the dura but not to the brain of rats with uncompromised blood brain barrier',
359 *Cephalalgia*, 40: 229-40.

360 Paige, C., I. Plasencia-Fernandez, M. Kume, M. Papalampropoulou-Tsiridou, L. E. Lorenzo, E. T.
361 David, L. He, G. L. Mejia, C. Driskill, F. Ferrini, A. L. Feldhaus, L. F. Garcia-Martinez, A. N.
362 Akopian, Y. De Koninck, G. Dussor, and T. J. Price. 2022. 'A Female-Specific Role for
363 Calcitonin Gene-Related Peptide (CGRP) in Rodent Pain Models', *J Neurosci*, 42: 1930-44.

364 Recober, A., A. Kuburas, Z. Zhang, J. A. Wemmie, M. G. Anderson, and A. F. Russo. 2009. 'Role of
365 calcitonin gene-related peptide in light-aversive behavior: implications for migraine', *J Neurosci*,
366 29: 8798-804.

367 Russo, A. F. 2015. 'Calcitonin gene-related peptide (CGRP): a new target for migraine', *Annu Rev*
368 *Pharmacol Toxicol*, 55: 533-52.

369 Tian, R., Y. Zhang, Q. Pan, Y. Wang, Q. Wen, X. Fan, G. Qin, D. Zhang, L. Chen, Y. Zhang, and J.
370 Zhou. 2022. 'Calcitonin gene-related peptide receptor antagonist BIBN4096BS regulates
371 synaptic transmission in the vestibular nucleus and improves vestibular function via
372 PKC/ERK/CREB pathway in an experimental chronic migraine rat model', *J Headache Pain*, 23:
373 35.

374 Zhang, Y., Y. Zhang, K. Tian, Y. Wang, X. Fan, Q. Pan, G. Qin, D. Zhang, L. Chen, and J. Zhou. 2020.
375 'Calcitonin gene-related peptide facilitates sensitization of the vestibular nucleus in a rat model
376 of chronic migraine', *J Headache Pain*, 21: 72.

377

378

379

Fig. 1:

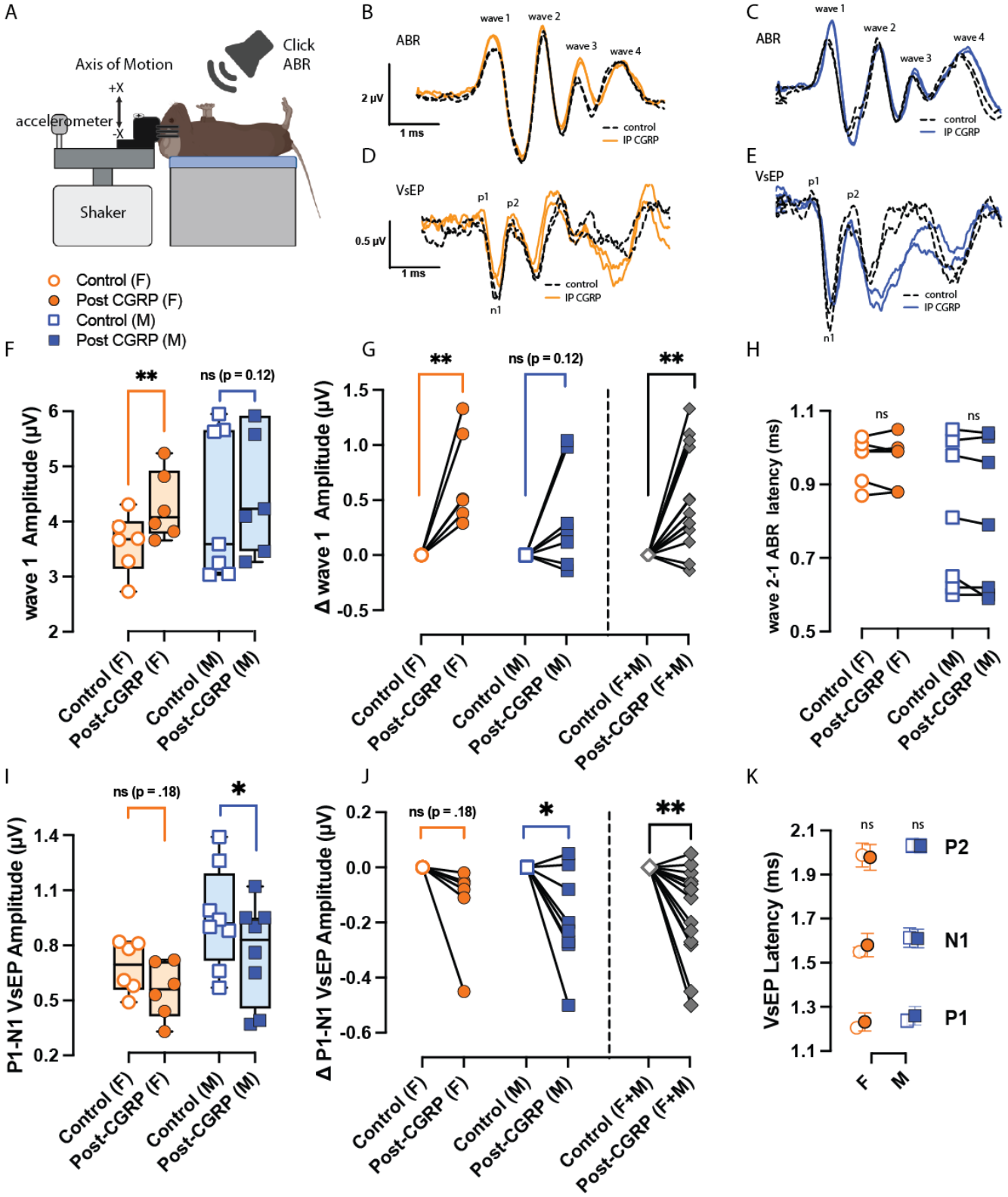
A
Click
ABR
Axis of Motion
+X
-X
accelerometer
Shaker
Control (F)
Post CGRP (F)
Control (M)
Post CGRP (M)
B
ABR
wave 1
wave 2
wave 3
wave 4
2 µV
1 ms
control
IP CGRP
C
ABR
wave 1
wave 2
wave 3
wave 4
control
IP CGRP
D
VsEP
p1
p2
n1
0.5 µV
1 ms
control
IP CGRP
E
VsEP
p1
p2
n1
control
IP CGRP
F
wave 1 Amplitude (µV)
**
ns (p = 0.12)
Control (F)
Post-CGRP (F)
Control (M)
Post-CGRP (M)
G
Δ wave 1 Amplitude (µV)
**
ns (p = 0.12)
**
Control (F)
Post-CGRP (F)
Control (M)
Post-CGRP (M)
Control (F+M)
Post-CGRP (F+M)
H
wave 2-1 ABR latency (ms)
ns
ns
Control (F)
Post-CGRP (F)
Control (M)
Post-CGRP (M)
I
P1-N1 VsEP Amplitude (µV)
ns (p = .18)
*
Control (F)
Post-CGRP (F)
Control (M)
Post-CGRP (M)
J
Δ P1-N1 VsEP Amplitude (µV)
ns (p = .18)
*
**
Control (F)
Post-CGRP (F)
Control (M)
Post-CGRP (M)
Control (F+M)
Post-CGRP (F+M)
K
VsEP Latency (ms)
ns
ns
P2
N1
P1
F
M

Fig. 2:

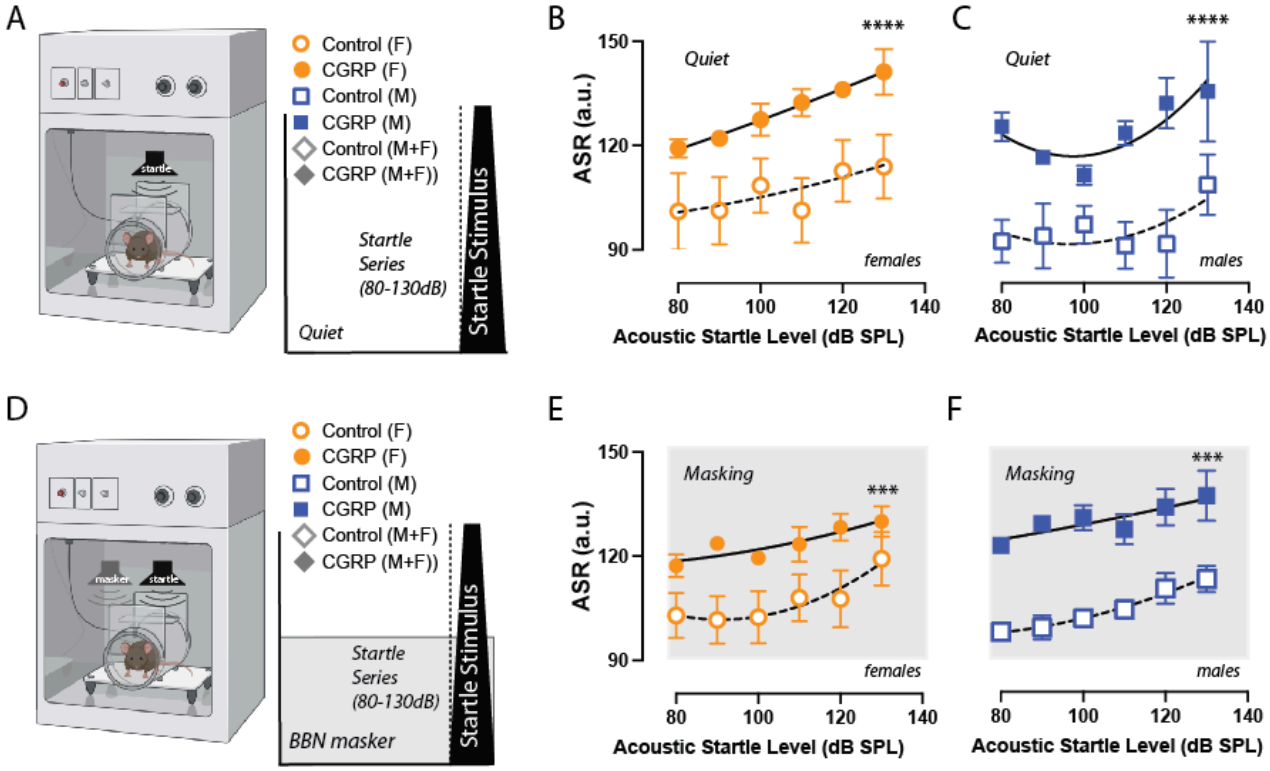
A
Control (F)
CGRP (F)
Control (M)
CGRP (M)
Control (M+F)
CGRP (M+F))
Startle Series (80-130dB)
Quiet
Startle Stimulus
B
Quiet
****
ASR (a.u.)
150
120
90
females
80
100
120
140
Acoustic Startle Level (dB SPL)
C
Quiet
****
males
Acoustic Startle Level (dB SPL)
D
Control (F)
CGRP (F)
Control (M)
CGRP (M)
Control (M+F)
CGRP (M+F))
Startle Series (80-130dB)
BBN masker
Startle Stimulus
E
Masking
***
ASR (a.u.)
150
120
90
females
Acoustic Startle Level (dB SPL)
F
Masking
***
males
Acoustic Startle Level (dB SPL)

Fig. 3:

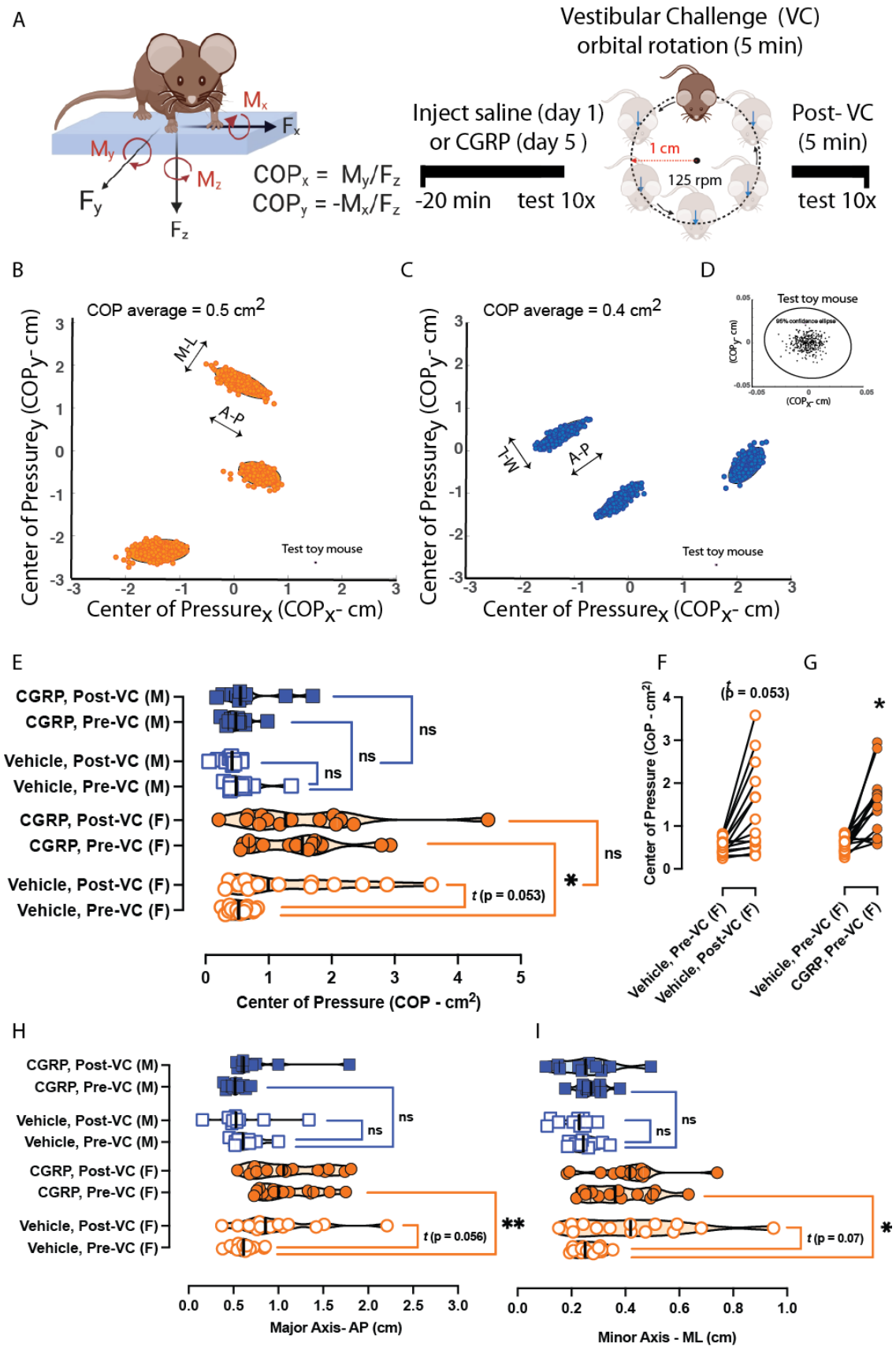
A
Vestibular Challenge (VC)
orbital rotation (5 min)
Inject saline (day 1)
or CGRP (day 5)
-20 min
test 10x
1 cm
125 rpm
Post- VC
(5 min)
test 10x
M_x
F_x
M_y
M_z
F_y
F_z
$COP_x = M_y/F_z$
$COP_y = -M_x/F_z$
B
COP average = 0.5 cm^2
M-L
A-P
Test toy mouse
Center of Pressure$_y$ (COP$_y$- cm)
Center of Pressure$_x$ (COP$_x$- cm)
C
COP average = 0.4 cm^2
M-L
A-P
Test toy mouse
D
Test toy mouse
95% confidence ellipse
E
CGRP, Post-VC (M)
CGRP, Pre-VC (M)
Vehicle, Post-VC (M)
Vehicle, Pre-VC (M)
CGRP, Post-VC (F)
CGRP, Pre-VC (F)
Vehicle, Post-VC (F)
Vehicle, Pre-VC (F)
ns
t (p = 0.053)
Center of Pressure (COP - cm^2)
F
(p = 0.053)
Center of Pressure (CoP - cm^2)
Vehicle, Pre-VC (F)
Vehicle, Post-VC (F)
G
Vehicle, Pre-VC (F)
CGRP, Pre-VC (F)
H
t (p = 0.056)
Major Axis- AP (cm)
I
t (p = 0.07)
Minor Axis - ML (cm)

398 **Figure Legends:**

399 **Fig. 1: A.** Schematic illustrating mouse setup for VsEP/ABR recordings captured during baseline
400 (control) and 20-30 minutes after intraperitoneal (IP) injections of either PBS vehicle or 0.1 mg/kg
401 CGRP in male (M) and female (F) C57BL6/J mice**. B-C**. Representative click-evoked ABR waveforms -
402 in duplicate -were collected for ABR at a maximal intensity of 100 dB SPL, and waves were labeled
403 (wave1 – wave 4). **D-E.** Likewise, representative VsEP waveforms were collected at +6 dB re: 1 g/ms
404 having three, labeled response peaks (p1, n1, and p2). Orange and blue colors are used to distinguish
405 female and male tracings post-CGRP, respectively. Whisker (**F, I**) and before-after (**G, H, J, K**) plots
406 are used to show changes in amplitude and latencies for ABR and VsEP recordings, and the following
407 symbols and colors are used: female control (open, orange circle), female post-CGRP (closed, orange
408 circle), male control (open, blue square), male post-CGRP (closed, blue square). **F-G**. A statistically
409 significant increase is seen in female wave 1 ABR amplitude post-CGRP ($p = 0.007$), and also when
410 sexes are pooled ($p = 0.002$). **I-J.** For VsEPs, a statistically significant decrease in P1-N1 VsEP
411 amplitudes is seen in males ($p = 0.02$) and when sexes are pooled ($p = 0.003$). **H, K.** IP CGRP had no
412 significant effects on ABR or VsEP latencies.

413

414 **Fig. 2: Systemic CGRP increases Acoustic Startle Responses (ASR) in both quiet and**
415 **background noise, suggesting increased sound sensitivity. A.** Schematic of startle stimulus
416 presented in otherwise quiet background conditions. **B.C**. For female mice (**B**, n=6), and male mice (**C**,
417 n=6), there were significant differences between vehicle and IP injected CGRP ASR measures in quiet
418 conditions ($p<0.0001$). All mice were more sensitive to the same sound level of ASR stimulus after
419 being injected with CGRP. **D.** Schematic of startle stimulus embedded in continuous 60dB SPL
420 broadband background noise. **E. F.** Again, ASR embedded in noise was also more sensitive to same
421 sound level after CGRP injection as shown for female mice (**E**, n=6), male mice (**F**, n=6), ($p<0.001$). All
422 mice were more sensitive to the same level of ASR stimulus whether delivered in quiet or in BBN after
423 being injected with CGRP. Moreover, all mice show ASR increases with sound level from 80 to 130dB
424 SPL with near maximal startle is elicited by 130 dB SPL stimulus levels. Error bars are SEMs.

425

426 **Fig. 3: CGRP and VC's effects on postural sway.** Figures are graphically depicted in the following
427 manner: vehicle control (open circle), CGRP (closed circle), female (orange) and male (blue). (A) The
428 assay timeline involved mice being assessed for effects of IP vehicle control (saline) or IP CGRP on
429 day 1 or day 5, respectively. A 5-minute orbital rotation (125 rpm for 5 minutes, orbital radius = 1 cm)
430 was used as the vestibular challenge. **(B and C)** Group 95% ellipse areas during pre-VC testing were
431 computed to be 0.50 ± 0.06 cm^2 for females and 0.4 ± 0.04 cm^2 for males. **(D)** A toy mouse was
432 measured to be 0.02 ± 0.0005 cm^2 for comparison with live animals. **(E)** Violin plot graphically depicts
433 the distribution of average 95% ellipse areas across sex and treatment and Tukey post-hoc analysis
434 was used to determine significant differences, which were also shown in before/after plots. During pre-
435 VC tests, females had higher 95% ellipse areas compared to males by 0.96 ± 0.19 cm^2 ($p = 0.007$). (**F**)
436 The before-after plot shows a trend (*t(p=0.053)*) for female mice to exhibit greater sway after vestibular
437 challenge with vehicle injection. **(G)** Before-after plot shows during pre-VC testing in females, IP CGRP
438 caused increased 95% ellipse areas by 0.94 ± 0.23 cm^2 when compared to their IP vehicle (p
439 $= 0.01$). **(H)** For Pre-VC AP sway in females, IP CGRP increased AP ellipse lengths by 0.49 + 0.10 cm
440 compared to IP vehicle ($p = 0.005$). A marginal increase in female AP lengths was detected in IP
441 vehicle from pre-VC to post-VC, but this was trending *(t (p = 0.056)*). **(I)** For Pre-VC ML sway in
442 females, IP CGRP increased ML ellipse lengths by 0.12 + 0.03 cm compared to IP vehicle, ($p = 0.02$).
443 In IP-vehicle treated females, an increase (trend) in ML ellipse lengths is observed from pre-VC to post-
444 VC (*t (p = 0.07*)). IP CGRP-treated females had higher AP lengths compared to males during pre-VC
445 by 0.57 + 0.10 cm, ($p = 0.0002$), but this sex-specific difference was not seen in ML lengths.
446
447